Proposal for gravitational-wave detection beyond the standard quantum limit through EPR entanglement

Ma, Yiqiu; Miao, Haixing; Heyun Pang, Belinda; Evans, Matthew; Zhao, Chunnong; Harms, Jan; Schnabel, Roman; Chen, Yanbei

DOI:
10.1038/nphys4118

Proposal for Gravitational-Wave Detection Beyond the Standard Quantum Limit using EPR Entanglement

Yiqiu Ma,[1] Haixing Miao,[2] Belinda Heyun Pang,[1] Matthew Evans,[3] Chunnong Zhao,[4] Jan Harms,[5,6] Roman Schnabel,[7] and Yanbei Chen[1]

[1] *Theoretical Astrophysics 350-17, California Institute of Technology, Pasadena, CA 91125, USA*
[2] *School of Physics and Astronomy, University of Birmingham, Birmingham, B15 2TT, United Kingdom*
[3] *Massachusetts Institute of Technology, Cambridge, Massachusetts 02139, USA*
[4] *School of Physics, University of Western Australia, Western Australia 6009, Australia*
[5] *Università degli Studi di Urbino "Carlo Bo", I-61029 Urbino, Italy*
[6] *INFN, Sezione di Firenze, Firenze 50019, Italy*
[7] *Institut für Laserphysik and Zentrum für Optische Quantentechnologien, Universität Hamburg, Luruper Chaussee 149, 22761 Hamburg, Germany*

(Dated: March 15, 2017)

The Standard Quantum Limit in continuous monitoring of a system is given by the trade-off of shot noise and back-action noise. In gravitational-wave detectors, such as Advanced LIGO, both contributions can simultaneously be squeezed in a broad frequency band by injecting a spectrum of squeezed vacuum states with a frequency-dependent squeeze angle. This approach requires setting up an additional long base-line, low-loss filter cavity in a vacuum system at the detector's site. Here, we show that the need for such a filter cavity can be eliminated, by exploiting EPR-entangled signal and idler beams. By harnessing their mutual quantum correlations and the difference in the way each beam propagates in the interferometer, we can engineer the input signal beam to have the appropriate frequency dependent conditional squeezing once the out-going idler beam is detected. Our proposal is appropriate for all future gravitational-wave detectors for achieving sensitivities beyond the Standard Quantum Limit.

Detection of gravitational waves from merging binary black holes (BBH) by the Laser Interferometer Gravitational-wave Observatory (LIGO) opened the era of gravitational wave astronomy [1]. The future growth of the field relies on the improvement of detector sensitivity, and the vision for ground-based gravitational-wave detection is to improve, eventually by a factor $\sim$30 in amplitude in the next 30 years [2–6]. This will eventually allow us to observe all BBH mergers that take place in the universe, thereby inform on the formation mechanism of BBH, the evolution of the universe [5, 7], and the way gravitational waves propagate through the universe [8, 9]. Higher signal-to-noise ratio observations of BBH will allow demonstrations and tests of effects of general relativity in the strong gravity and nonlinear regimes [10, 11]. Besides BBH, gravitational waves from neutron stars are being highly anticipated, as well as an active program of joint EM-GW observations [12, 13]. Finally, improved sensitivity may lead to detections of more exotic sources [14], as well as surprises.

A key toward better detector sensitivity is to suppress *quantum noise*, which arises from the quantum nature of light and the mirrors, and is driven by vacuum fluctuations of the optical field entering from the dark port of the interferometer [15–18]. There are two types of quantum noise: shot noise, the finite displacement resolution due to the finite number of photons, and the radiation-pressure noise, which arises from the photons randomly impinging on the mirrors. In the broadband configuration of Advanced LIGO, we measure the phase quadrature of the carrier field at the dark port, the quadrature that contains GW signal. In this case, shot noise is driven by phase fluctuations of the incoming optical field, while radiation-pressure noise is driven by amplitude fluctuations. The trade off between these two types of noise, as dictated by the Heisenberg Uncertainty Principle, gives rise to a sensitivity limitation called the Standard Quantum Limit (SQL) [19–21].

One way to improve LIGO's sensitivity with minimal modification to its optical configuration is to inject squeezed vacuum into the dark port [18, 22–24]. More than 10 dB of squeezing down to audio side-band frequency (10 Hz to 10 kHz) has been demonstrated in the lab [25–30], while moderate noise reductions have been demonstrated in the large-scale interferometers GEO 600 [31] and LIGO [32]. However, squeezed vacuum generated by a nonlinear crystal via Optical Parametric Amplification (OPA) is frequency-independent for audio sidebands: within the GW band, we can only "squeeze" a fixed quadrature — fluctuations in the orthogonal quadrature are amplified by the same factor, as required by the Heisenberg Uncertainty Principle. This does not allow broadband improvement of sensitivity beyond the SQL [19, 33] such as the example shown in Fig. 1; instead, a frequency-dependent quadrature must be squeezed for each sideband frequency. Starting off from frequency-independent squeezing, we must *rotate* the squeezed quadrature in a frequency-dependent way [19, 34]; for the broadband configuration of Advanced LIGO, this rotation angle needs to gradually transition by $\pi/2$ at a frequency scale of 50 Hz [35]. Kimble *et al.* [19] proposed to achieve such rotation by filtering the field with two Fabry-Perot cavities; Khalili further showed that it is often sufficient to use one cavity with bandwidth and de-

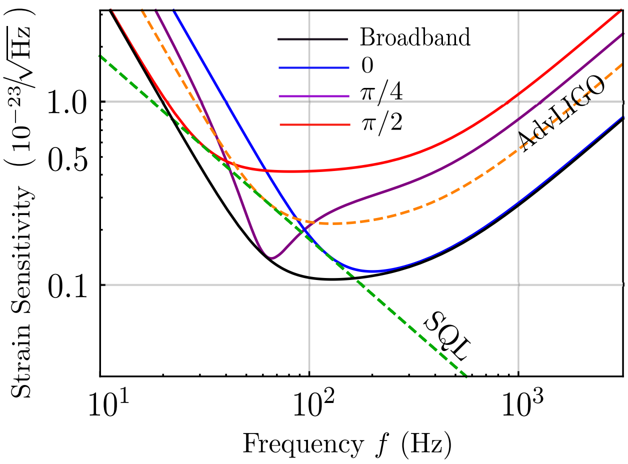

FIG. 1: Sensitivity of a AdvLIGO type gravitational wave detector driven by squeezed vacuum (6 dB squeeze degree is chosen for comparing the 5% input/output loss case in Fig. 4) with a fixed squeezing angle. The red, purple and blue curves describe the cases when squeezed light is injected with squeezing angle 0(corresponding to an amplitude squeezed vacuum), $\pi/4$ and $\pi/2$, respectively. The black curve is the case when there is a frequency dependent squeezed vacuum injection.

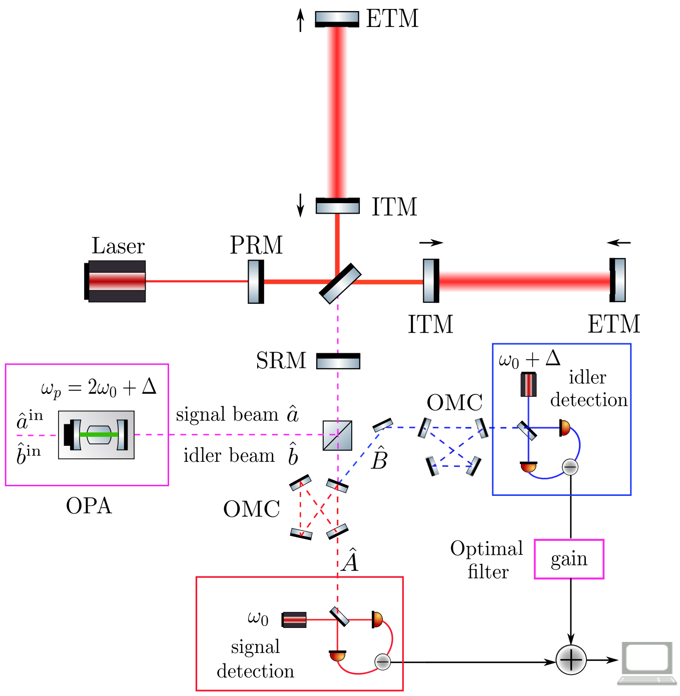

FIG. 2: Optical configuration for noise suppression via EPR entanglement. The OPA is detuned by Δ, generating signal beam a and idler beam b and injecting them into the interferometer. Upon returning from the interferometer, signal beam A and idler beam B are separated and filtered by the output mode cleaners (denoted as OMC in the figure), and each detected via homodyne detection. Measurement data are combined using an optimal filter for obtaining the squeezing of the quantum noise on the signal channel. The abbreviations PRM, ITM, ETM and SRM stand for power recycling mirror, input test mass mirror, end test mass mirror and signal recycling mirror, respectively.

tuning (from the carrier frequency) roughly at the transition frequency [36, 37]. However, the narrowness of the bandwidth requires the filter cavity to be long in order to limit impact from optical losses; the current plan for Advanced LIGO is to construct a $\sim 16\,$m filter cavity [35, 38, 39], and $\sim$ 300m long cavities have been studied for KAGRA [40] and for the Einstein Telecscope [41]. Alternative theoretical proposals for creating narrow-band filter cavities were also discussed, they are strongly limited by thermal noise and/or optical losses [42–44].

In this paper, we propose a novel strategy to achieve broadband squeezing of the total quantum noise via the preparation of EPR entanglement and the dual use of the interferometer as both the GW detector and the filter, eliminating the need for external filter cavities.

As shown in Fig. 2, our strategy is divided into 4 steps. (i) We detune the pumping frequency of the OPA away from $2\omega_0$ (where ω_0 is the carrier frequency of the interferometer) to $\omega_p = 2\omega_0 + \Delta$, with Δ an rf frequency of a few MHz, creating two EPR-entangled beams: the *signal beam* around the carrier frequency ω_0, and the *idler beam* around $\omega_0 + \Delta$. (ii) The idler beam, being far detuned from the carrier, sees the interferometer as a simple detuned cavity, and experiences frequency-dependent quadrature rotation, see Fig. 3, which can be optimised by adjusting Δ with respect to the lengths of interferometer cavities. (iii) When traveling out of the interferometer, the collinear signal and idler beams are separated and filtered by the output mode cleaners and measured by beating with local oscillators at frequencies ω_0 and $\omega_0 + \Delta$, respectively. (iv) The homodyne measurement of a fixed quadrature of the out-going idler beam conditionally squeezes the *input signal beam* in a frequency dependent way, thereby achieving the broadband reduction of quantum noise. Practically, benefit of the conditional squeezing of the signal beam is obtained as we apply a Wiener filter to the photocurrent of the idler and subtract it from the photocurrent of the signal beam. Without optical losses, using parameters in Table I (with a 15 dB squeezed vacuum in particular), we obtain the solid black curve in Fig. 4, with ∼11-12 dB improvement over the entire frequency band. We shall next discuss more details of the configuration, as well as the impact of optical losses; further details are provided in Supplementary Materials.

EPR entanglement by detuning the OPA.– For an OPA pumped at ω_p, it is often convenient to study *quadrature fields* around $\omega_p/2$, which are linear combinations of upper and lower sideband fields at $\omega_p/2 \pm \Omega$, with ζ quadrature defined by:

$$\hat{c}_\zeta(\Omega) = \left(e^{-i\zeta}\hat{c}_{\omega_p/2+\Omega} + e^{+i\zeta}\hat{c}^\dagger_{\omega_p/2-\Omega}\right)/\sqrt{2} \qquad (1)$$

Here $\hat{c}_\omega$ and $\hat{c}^\dagger_\omega$ are the annihilation and creation operators for the optical field at ω; we will use $\hat{c}_{1,2}$ to stand for

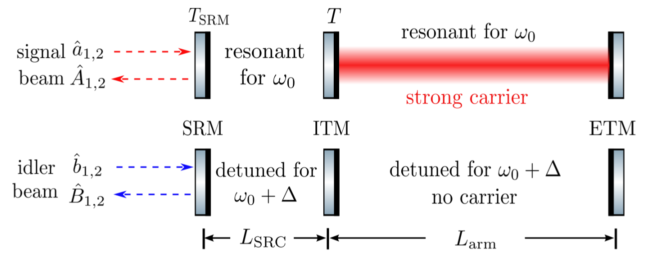

FIG. 3: The differential mode of the interferometer as seen by the signal (upper panel) and idler (lower panel) beams.

λ	Carrier laser wavelength	1064 nm
$T_{\rm SRM}$	SRM power transmissivity	0.35
T	ITM power transmissivity	0.014
$L_{\rm arm}$	Arm cavity length	$\sim$ 4 km
$L_{\rm SRC}$	Signal recycling cavity length	$\sim$ 50 m
γ	Detection bandwidth	389 Hz
m	Mirror mass (ITM and ETM)	40 kg
I_c	Intra cavity power	650 kW
Δ	Idler-signal detuning	-15.3 MHz
r	Squeeze factor of the OPA	1.23 (15 dB)

TABLE I: Sample Parameters for Advanced LIGO. (See supplementary material for details.)

$\hat{c}_{0,\pi/2}$, and $\hat{c}_\zeta = \hat{c}_1 \cos\zeta + \hat{c}_2 \sin\zeta$. For a squeeze factor r and squeeze angle θ, the orthogonal quadratures $\hat{c}_\theta$ and $\hat{c}_{\theta+\pi/2}$ have uncorrelated fluctuations, with spectra given by

$$S_{\hat{c}_\theta \hat{c}_\theta} = e^{-2r}\,,\; S_{\hat{c}_{\theta+\pi/2}\hat{c}_{\theta+\pi/2}} = e^{+2r}\,. \qquad (2)$$

Compared with vacuum, fluctuations in $\hat{c}_\theta$ are suppressed by e^{2r}, and those in $\hat{c}_{\theta+\pi/2}$ are amplified by e^{2r}. This is due to the entanglement between the upper and lower sidebands, $\omega_p/2 \pm \Omega$, generated by the optical nonlinearity. However, any pair of sideband fields with frequencies ω_1 and ω_2 within the squeeze bandwidth (usually >MHz) from $\omega_p/2$, and satisfying $\omega_1+\omega_2=\omega_p$, are entangled; in particular, for the proposed OPA (Fig. 2) with pumping frequency $\omega_p = 2\omega_0+\Delta$, we have entanglement between $\omega_0+\Omega$ and $\omega_0+\Delta-\Omega$, as well as $\omega_0-\Omega$ and $\omega_0+\Delta+\Omega$, as shown in the upper panel of Fig. 5. As it turns out, this entanglement is equivalent to an EPR-type entanglement [45–47] between quadratures around ω_0 [consisting of $\omega_0 \pm \Omega$ sidebands, denoted by $\hat{a}_\zeta(\Omega)$] and those around $\omega_0+\Delta$ [consisting $\omega_0+\Delta\pm\Omega$ sidebands, denoted by $\hat{b}_\zeta(\Omega)$]. In terms of the four fields, $(\hat{a}_1 \pm \hat{b}_1)/\sqrt{2}$ and $(\hat{a}_2 \pm \hat{b}_2)/\sqrt{2}$, they are mutually uncorrelated, and have spectra

$$S_{(\hat{a}_1\pm\hat{b}_1)/\sqrt{2}} = e^{\pm 2r}\,, \quad S_{(\hat{a}_2\pm\hat{b}_2)/\sqrt{2}} = e^{\mp 2r}\,. \qquad (3)$$

In other words, for $r \gtrsim 1$, fluctuations in $\hat{b}_1 - \hat{a}_1$ and $\hat{b}_2 + \hat{a}_2$ are both much below vacuum level, as in the original EPR situation. In this way (lower panel of

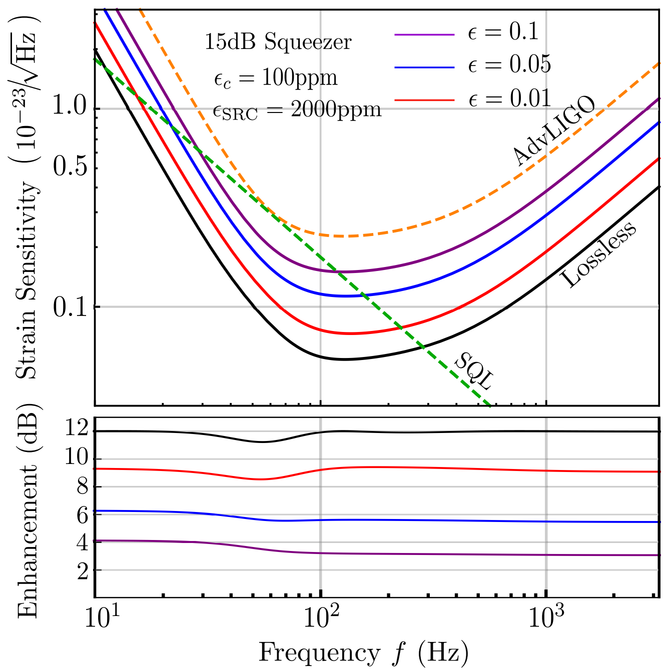

FIG. 4: Upper panel: Noise spectrum of Advanced LIGO configurations with conditional frequency-dependent squeezing by using a 15 dB squeezed vacuum at MHz frequencies(see Table I), assuming no loss (black), and assuming arm-cavity loss $\epsilon_c = 100$ ppm and signal recycling cavity loss $\epsilon_{\rm SRC} = 2000$ ppm, plus an identical input and output loss ϵ of 1% (red), 5% (blue) and 10% (purple). Lower panel: The sensitivity improvement factor measured in terms of dB.

Fig. 5), if we detect $\hat{b}_\theta = \hat{b}_1 \cos\theta + \hat{b}_2 \sin\theta$, we can predict $\hat{a}_{-\theta} = \hat{a}_1 \cos\theta - \hat{a}_2 \sin\theta$ with a very good accuracy, while not providing any information for $\hat{a}_{\pi/2-\theta}$. More precisely, given measurement data of the idler quadrature $\hat{b}_\theta$, the signal beam will be conditionally squeezed, with *conditional spectra*

$$S^{|\hat{b}_\theta}_{\hat{a}_{-\theta}\hat{a}_{-\theta}} = 1/\cosh(2r)\,,\; S^{|\hat{b}_\theta}_{\hat{a}_{\frac{\pi}{2}-\theta}\hat{a}_{\frac{\pi}{2}-\theta}} = \cosh(2r)\,, \qquad (4)$$

where the squeeze angle is $-\theta$, and the squeeze factor is $(\log\cosh(2r))/2$. For significant squeezing, $e^{2r} \gg 1$, this corresponds to 3 dB less squeezing than before detuning the pump field.

Improvement of Detector Sensitivity.– As shown in Fig.1, after signal beam $\hat{a}_{1,2}$ and idler beam $\hat{b}_{1,2}$ are fed into the interferometer, we detect phase quadratures of the out-going signal and the idler beams, A_2 and B_2, after they are separated and filtered by the output mode cleaners (Fig. 2). For the signal beam (upper panel of Fig. 3), we have [19]:

$$\hat{A}_2 = e^{2i\beta}(\hat{a}_2 - \mathcal{K}\hat{a}_1) + \sqrt{2\mathcal{K}} e^{i\beta} h/h_{\rm SQL}\,, \qquad (5)$$

which consists of shot noise, radiation-pressure noise, and signal, with $\beta = \arctan(\Omega/\gamma)$, where γ is the bandwidth of the interferometer seen by the signal beam,

$$h^2_{\rm SQL} = 8\hbar/(m\Omega^2 L^2), \quad \mathcal{K} = 2\Theta^3\gamma/[\Omega^2(\Omega^2+\gamma^2)], \quad (6)$$

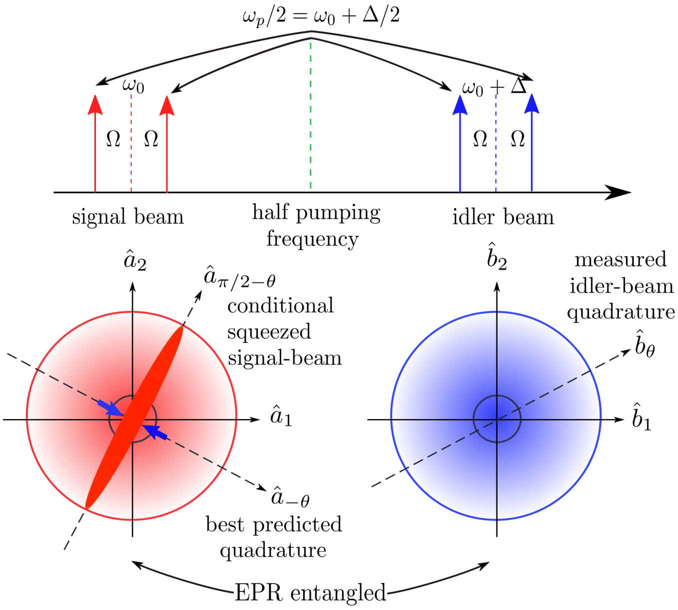

FIG. 5: Spectral decomposition of EPR-entangled beams (upper panel) and the quantum statics of the signal and idler beams (lower panel).

and $\Theta = [8\omega_0 I_c/(mLc)]^{1/3}$.

Here we need to squeeze the $a_{[-\arctan(1/\mathcal{K})]}$ quadrature of the input signal beam, which requires detecting $b_{\arctan(1/\mathcal{K})}$. If we detect B_2, we will need the interferometer (lower panel of Fig. 3) to apply a rotation of $\Phi_{\rm rot} = \arctan\mathcal{K}$ to the idler beam so that $\hat{B}_2 = \hat{b}_{\arctan(1/\mathcal{K})}$. This can be realized approximately by adjusting the detuning Δ and the length of signal-recycling cavity and arm cavity (see Supplementary Material for details), if $\Theta \ll \gamma$. To achieve the sensitivity provided by conditional squeezing, we need to compute the best estimate of $\hat{A}_2$ from $\hat{B}_2$, and subtract it from $\hat{A}_2$. If a rotation by $\Phi_{\rm rot}$ is realized exactly, we will have a noise spectrum of

$$S_h \approx \frac{h^2_{\rm SQL}}{2\cosh 2r}\left(\mathcal{K} + \frac{1}{\mathcal{K}}\right), \tag{7}$$

where conditional squeezing provides a cosh $2r$ suppression. In reality, we get less suppression since the interferometer, acting as a single cavity, does not exactly realize $\Phi_{\rm rot}$ for the idler beam. In Fig. 4, the black curve shows the actual noise spectrum for parameters in Table I.

Discussions.– In Fig. 4, we plot noise spectra of interferometers with optical losses. In particular, we include losses in the arm cavities, at the input port, and during readout. As it turns out, the current 100 ppm arm cavity loss and 2000 ppm signal recycling cavity loss [48] has only a small effect on the noise (for details, see Supplementary Material). When the input loss and the readout loss are both around 10%, the sensitivity improvement is only roughly 3 dB, which corresponds to an amplitude improvement ~ 1.4. However, for a lower loss of 5%, which is promising in the near future [35, 48, 49], we can gain $\sim$ 6 dB or a factor of $\sim$ 2 improvement in amplitude. This corresponds to an increase of sensitive sky volume by a factor of 8. Compared to the traditional scheme with a filter cavity [35], our input and detection losses are doubled, because signal and idler beams experience the same amount of loss during propagation. Although we do suffer less from loss in the filter cavity compare to the design based on an auxiliary filter cavity (since arm cavities have less loss), this higher level of input and detection losses is the price we have to pay in this scheme for eliminating the additional filter cavity.

Acknowledgements.– Research of Y.M, B.H.P, Y.C is supported by NSF grant PHY-1404569 and PHY-1506453, as well as the Institute for Quantum Information and Matter, a Physics Frontier Center. H.M. is supported by the Marie-Curie Fellowship and UK STFC Ernest Rutherford Fellowship. C.Z. would like to thank the support of Australian Research Council Discovery Project DP120104676 and DP120100898. R.S. is supported by DFG grant SCHN757/6 and by ERC grant 339897 ('Mass Q').

Author contributions.– Y. M., H. M. and Y. C. formulated the idea; Y. M. did the analysis of the idea and wrote the initial draft, which was later revised by Y. C; B. P. checked Y. M's calculation; M. E., J. H., R. S and C. Z. provided important experimental parameters for doing theoretical analysis and gave valuable comments on Y. M's calculations and initial/revised draft.

[1] Abbott, B. (et al.). Observation of Gravitational Waves from a Binary Black Hole Merger. *Physical Review Letters*, **116** (061102), (2016).

[2] Punturo, M. (et al.). The Einstein Telescope: a third-generation gravitational wave observatory. *Classical and Quantum Gravity*, **27** (19), (2010).

[3] Danilishin, S. and Khalili, F. Ya. Quantum Measurement Theory in Gravitational-Wave Detectors. *Living Review in Relativity*, **15** (5), (2012).

[4] Miao, H., Yang, H., Adhikari, R. X. and Chen, Y. Quantum limits of interferometer topologies for gravitational radiation detection. *Classical Quantum Gravity*, **31** (16), (2014).

[5] Dwyer, S., Sigg, D., Ballmer, S., Barsotti, L., Mavalvala, N., and Evans. M. Gravitational wave detector with cosmological reach. *Physical Review D*, **91** (082001), (2015).

[6] Abbott, B. (et al.). Exploring the sensitivity of next generation gravitational wave detectors. *LIGO Document*, (P1600143-v14), (2016).

[7] Sathyaprakash, B. (et. al). Scientific objectives of Einstein Telescope. *Classical and Quantum Gravity*, **29** (12), (2012).

[8] Tso, R., Isi, M., Chen, Y., and Stein, L. Modeling the dispersion and polarization content of gravitational waves for tests of general relativity. In *Seventh Meeting on CPT and Lorentz Symmetry*, (2016).

[9] Kostelecky, A. and Mewes, M. Testing local Lorentz invariance with gravitational waves. *Physics Letters B*, **757**: 510–514, (2016).

[10] Lasky, P., Thrane, E., Levin, Yu., Blackman, J. and Chen, Y. Detecting gravitational-wave memory with ligo: implications of gw150914. *Physical Review Letters*, **117** (061102), (2016).

[11] Berti, E. Astrophysical Black Holes as Natural Laboratories for Fundamental Physics and Strong-Field Gravity. *Brazilian Journal of Physics*, **43** (341), (2013).

[12] Chu, Q., Howell, E. J., Rowlinson, A., Gao, H., Zhang, B., Tingay, S. J., Boër, M., and Wen, L. Capturing the electromagnetic counterparts of binary neutron star mergers through low-latency gravitational wave triggers. *Monthly Notices of the Royal Astronomical Society*, **459**: 121–139, (2016).

[13] Metzger, B. D., and Berger, E. What is the most promising electromagnetic counterpart of a neutron star binary merger? *The Astrophysical Journal*, 746(1):**48**, (2012).

[14] Aasi, J. (et. al). Constraints on Cosmic Strings from the LIGO-Virgo Gravitational-Wave Detectors. *Physical Review Letters*, **112** (131101), 2014.

[15] Drever, R. W. P., Hough, J., Edelstein, W. A., Pugh, J. R., and Martin, W. In B. Bertotii, editor, *Experimental Gravitation*, page **365**, Pavia, Italy., (1976). Accademia Nazionale dei Lincei.

[16] Braginsky, V. B, and Vorontsov, Yu. I. *Uspekhi Fizicheskikh Nauk*, **114** (41), (1974).

[17] Weiss, R. *Sources of Gravitational Radiation.* Cambridge University Press, (1979).

[18] Caves, C. M. Quantum-mechanical noise in an interferometer. *Physical Review D*, **23** (1693), (1981).

[19] Kimble, H. J., Levin, Yu., Matsko, A. B., Thorne, K. S., and Vyatchanin, S. P. Conversion of conventional gravitational-wave interferometers into quantum nondemolition interferometers by modifying their input and/or output optics. *Physical Review D*, **65** (022002), (2001).

[20] Buonanno, A. and Chen, Y. Quantum noise in second generation, signal-recycled laser interferometric gravitational-wave detectors. *Physical Review D*, **64** (042006), (2001).

[21] Buonanno, A. and Chen, Y. Scaling law in signal recycled laser-interferometer gravitational-wave detectors. *Physical Review D*, **67** (062002), (2003).

[22] Unruh, W. G. *Quantum Noise in the Interferometer Detector*, page **647**. Plenum Press, New York, (1983).

[23] Schnabel, R., Mavalvala, N., McClelland, D. E. and Lam, P. K. Quantum metrology for gravitational wave astronomy. *Nature Communication*, **1** (121), (2010).

[24] LIGO Instrument Science White Paper. Technical report, Feb. (2015).

[25] Vahlbruch, H., Mehmet, M., Chelkowski, S., Hage, B., Franzen, A., Lastzka, N., Gossler, S., Danzmann, K., and Schnabel, R. Observation of Squeezed Light with 10-dB Quantum-Noise Reduction. *Physical Review Letters*, **100** (033602), (2009).

[26] Mehmet, M., Ast, S., Eberle, T., Steinlechner, S., Vahlbruch, H., and Schnabel, R. Squeezed light at 1550 nm with a quantum noise reduction of 12.3 dB. *Optics Express*, **19** (25763), (2011).

[27] Chua, S. S. Y., Stefszky, M. S., Mow-Lowry, C. M., Buchler, B. C., Dwyer, S., Shaddock, D. A., Lam, P. K., and McClelland, D. E. Backscatter tolerant squeezed light source for advanced gravitational-wave detectors. *Optics Letters*, **36** (23):4680–4682, (2011).

[28] Stefszky, M. S., Mow-Lowry, C. M., Chua, S. S. Y., Shaddock, D. A., Buchler, B. C., Vahlbruch, H., Khalaidovski, A., Schnabel, R., Lam, P. K., and McClelland, D. E. Balanced homodyne detection of optical quantum states at audio-band frequencies and below. *Classical Quantum Gravity*, **29** (145015), (2012).

[29] McKenzie, K., Grosse, N., Bowen, W. P., Whitcomb, S. E., Gray, M. B., McClelland, D. E., and Lam, P. K. Squeezing in the Audio Gravitational-Wave Detection Band. *Physical Review Letters*, **93** (161105), (2004).

[30] Vahlbruch, H., Mehmet, M., Danzmann, K., and Schnabel, R. Detection of 15 dB squeezed states of light and their application for the absolute calibration of photoelectric quantum efficiency. *Physical Review Letters*, **117** (110801), (2016).

[31] Abbott, B. (et al.). A gravitational wave observatory operating beyond the quantum shot-noise limit. *Nature Physics*, **7** (962), (2011).

[32] Abbott, B. (et al.). Enhanced sensitivity of the LIGO gravitational wave detector by using squeezed states of light. *Nature Photonics*, **7** (613), (2013).

[33] Jaekel, M. T., and Reynaud, S. Quantum Limits in Interferometer Measurement. *EPL (Europhysics Letters)*, **13** (4):301, (1990).

[34] Chelkowski, S., Vahlbruch, H., Hage, B., Franzen, A., Lastzka, N., Danzmann, K., and Schnabel, R. Experimental characterization of frequency-dependent squeezed light. *Physical Review A*, **71** (013806), (2005).

[35] Evans, M., Barsotti, L., Kwee, P., Harms, J. and Miao, H. Realistic filter cavities for advanced gravitational wave detectors. *Physical Review D*, **88** (022002), (2013).

[36] Khalili, F. Ya. Quantum variational measurement in the next generation gravitational-wave detectors. *Physical Review D*, **76** (102002), (2007).

[37] Khalili, F. Ya. Optimal configurations of filter cavity in future gravitational-wave detectors. *Physical Review D*, **81** (122002), (2010).

[38] Isogai, T., Miller, J., Kwee, P., Barsotti, L., and Evans, M. Loss in long-storage-time optical cavities. *Optics Express*, **21** (24):30114–30125, (2013).

[39] Kwee, P., Miller, J., Isogai, T., Barsotti, L., and Evans, M. Decoherence and degradation of squeezed states in quantum filter cavities. *Physical Review D*, **90** (062006), (2014).

[40] Caposcasa, E., Barsuglia, M., Degallaix, J., Pinard, L., Straniero, N., Schnabel, R., Somiya, K., Aso, Y., Tatsumi, D., and Flaminio, R. Estimation of losses in a 300 m filter cavity and quantum noise reduction in the kagra gravitational-wave detector. *Physical Review D*, **93** (082004), (2016).

[41] ET Science Team. Einstein gravitative wave telescope conceptual design study. *ET-0106C-10*, (2011).

[42] Mikhailov, E. E., Goda, K., Corbitt, T., and Mavalvala, N. Frequency-dependent squeeze-amplitude attenuation and squeeze-angle rotation by electromagnetically induced transparency for gravitational-wave interferometers. *Physical Review A*, **73** (053810), (2006).

[43] Ma, Y., Danilishin, S. L., Zhao, C., Miao, H., Korth, W. Z., Chen, Y., Ward, R. L., and Blair, D. G. Narrow-

ing the Filter-Cavity Bandwidth in Gravitational-Wave Detectors via Optomechanical Interaction. *Physical Review Letters*, **113** (151102), (2014).

[44] Qin, J., Zhao, C., Ma, Y., Chen, X., Ju, L., and Blair, D. G. Classical demonstration of frequency-dependent noise ellipse rotation using optomechanically induced transparency. *Physical Review A*, **89** (041802(R)), (2014).

[45] Zhang, J. Einstein-Podolsky-Rosen sideband entanglement in broadband squeezed light. *Physical Review A*, **67** (054302), (2003).

[46] Marino, A. M., Stroud, C. R., Wong, V., Bennink, R. S., and Boyd, R. W. Bichromatic local oscillator for detection of two-mode squeezed states of light. *Journal of the Optical Society of America B*, **24** (2):335–339, (2007).

[47] Hage, B., Samblowski, A., and Schnabel, R. Towards Einstein-Podolsky-Rosen quantum channel multiplexing. *Physical Review A*, **81** (062301), (2010).

[48] Barsotti, L. Ligo: The A+ Upgrade. *LIGO Document*, (G1601199-v2), (2016).

[49] Barsotti, L. Squeezing for Advanced LIGO. *LIGO Document*, G1401092-v1, (2014).